THE EFFECT OF DUST ON THE MARTIAN HADLEY CELLS IN THE PRESENCE OF TOPOGRAPHY AT EQUINOX.

A. M. Zalucha, *Massachusetts Institute of Technology, Cambridge, MA, USA (azalucha@mit.edu)***.**

Introduction

Several factors affect the boundaries and strengths of the Martian Hadley cells. The effects due to the change in the latitude of the subsolar point with season is well understood by application of terrestrial modeling studies (e.g. Lindzen and Hou, 1988). At equinox, in the absence of topography, the rising branch is located at the equator and the cells are of equal strength. As the latitude of the subsolar point is perturbed off of the equator, the summer cell becomes weaker and the winter cell becomes stronger. The rising branch moves into the summer hemisphere. Lindzen and Hou (1988) found that for a small change in the latitude of the subsolar point (in their case the latitude of maximum insolation), the change in the latitude of the rising branch was much larger. On Mars, without the moderating effect of an ocean with large heat storage capacity, the circulation at solstices is a single, cross-equatorial cell with broad areas of upwelling in the summer hemisphere and down welling at midlatitudes in the winter hemisphere.

Given the eccentric Martian orbit, one would expect the Hadley cell strength to be greater at L_s=270° than at 90°, since the heating is greater in the summer hemisphere, and in turn the latitudinal heating gradient that drives the Hadley circulation. Joshi et al. (1995) found that when the solar forcing was held constant between the two seasons, a factor of 1.5 difference in Hadley cell intensity was still present. Zalucha et al. (2010) showed that it was the north-south slope in the zonally averaged topography that caused the cell strength to decrease compared with fla topography at L_s=90°, but had little effect at L_s=270°. Richardson and Wilson (2002) showed that in the annual average, the asymmetry in the Hadley cells about the equator (in which the latitude of upwelling was located southward of the equator and the northern cell was stronger than the southern) was caused by the north-south slope and not the L_s of perihelion. Takahashi et al. (2003) showed that a similar asymmetry about the equator at equinox was caused by the north-south slope and not surface albedo or surface thermal inertia variations. Richardson and Wilson (2002), Takahashi et al. (2003), and Zalucha et al. (2010) showed that the slope was coupled to the atmosphere through convection, which changed the latitudinal gradient in heating that forces the Hadley circulation.

Basu et al. (2006) showed that at L_s=270°, as dust loading increased, the Hadley cell strength increased, while at L_s=90°, the strength also increased but by a larger amount. That is, the asymmetry between the solstices became less pronounced as dust loading increased. The contribution from the north-south slope apparently diminished as dust loading increased.

Here, I investigate the effect of high dust loading on the Hadley cells at equinox using a Mars general circulation model (MGCM). Cases with and without dust and with flat zonally averaged, and complete topography are compared.

Model

The dynamical core of the Massachusetts Institute of Technology (MIT) GCM solves the fundamental equations of geophysical flui dynamics in 3-D using the finit volume method on an Arakawa C-grid (Marshall et al., 1997). The model is hydrostatic and compressible. The atmosphere may exchange mass with the surface via a source/sink term in the continuity equation. The default configuratio has neither viscosity nor vertical diffusion, but uses an eighth-order Shapiro filte to remove numerical noise. The horizontal configuratio is a cube-sphere grid (Adcroft et al., 2004) with 32 × 32 points per cube face, equivalent to a resolution of 2.8° at the equator. This type of horizontal grid eliminates singularities at the poles that force horizontal winds to zero on a cylindrical grid projection. The vertical grid is an η coordinate (Adcroft and Campin, 2004) based in atmospheric pressure.

Zalucha et al. (2010) adapted the MIT GCM to Mars. Zero elevation corresponds to a pressure of 6 hPa, which is also used as a reference pressure elsewhere. The top level is centered at a pressure of 0.000117 hPa, which corresponds to a log pressure height of 119 km (using the reference pressure above and a scale height of 11 km). The top levels are not treated as realistically modeling the atmosphere in that region, since a sponge layer is also located in the upper levels. Mars Orbiter Laser Altimeter (MOLA; Smith et al., 1999) topography is used. Within each vertical level intersecting the surface, the resolution of the topography is increased by inserting sub grids spaced at 10% of the full vertical grid spacing at that level (Adcroft et al., 1997). Surface albedo and surface thermal inertia are constant. Boundary layer friction is specifie by a simple drag law and extends to a level at 70% of the surface pressure. The CO_2 mass cycle is not included, as its effect on the Hadley cells is not significan in our model. Instead, when the temperature falls below the CO_2 condensation temperature, it is instantenously returned back to the CO_2 condensation temperature.

The Zalucha et al. (2010) MIT MGCM has undergone revisions to the radiation scheme since Zalucha et al. (2010). Diurnally varying insolation is now used. The heating rate is now supplied directly instead of through Newtonian relaxation to a specif ed equilibrium temperature. The long wave heating is calculated using the semi-gray representation of the 15-μm band of Caballero et al. (2008). Shortwave dust heating at solar wavelengths is calculated using the δ-Eddington approximation for aerosol scattering (Briegleb, 1992). The single scattering albedo is 0.86, the phase function asymmetry parameter is 0.79, and the forward scattering fraction is 0.62 (Pollack et al., 1979). The dust mixing ratio q as a function of height is given by (Conrath, 1975)

$$q = q_o \exp\left[\nu\left(1 - \frac{p_{ref}}{p}\right)\right], \qquad (1)$$

where q_o is the mixing ratio at the reference pressure p_{ref}, p is pressure, and $\nu = 0.01$.

Results

The MGCM was run at L_s f xed at 0 for 120 sols; longer model runs show this time to be suff cient to obtain a steady state. The last 30 sols were time-averaged and analyzed. The solar optical depth at the surface was varied between 0 and 1. Three topographies were used—f at, zonally averaged MOLA topography, and complete zonally and meridional varying MOLA topography. Figure 1 shows the zonally averaged mass stream function for this set of runs. The left column (no dust) is the same conditions as the radiative-convective forcing case of Zalucha et al. (2010). For the case of f at topography, the cells are symmetric about the equator. The zonally averaged topography and complete topography cases shift the boundary between the cells southward, strengthen the northern cell, and weaken the southern cell. The qualitative similarity between zonally averaged topography and complete topography runs indicates that it is the north-south slope that is primarily responsible for the asymmetry in the cells. Zalucha et al. (2010) showed that the height of the surface was important in causing asymmetric Hadley cells about the equator because convection heated the atmosphere over an elevated surface more than at the same level over a lower surface. The meridionally varying topography changed the meridional heating gradient and consequently the relative strengths of each cell and the location of the boundary between them. Runs with the convection excluded (not shown) decoupled the surface from the atmosphere and the cells remained symmetric regardless of topography.

The right column of Fig. 1 shows the same experiments as Zalucha et al. (2010) but with the solar optical depth at the surface set to 1. The f at topography case produces symmetric cells, while the zonally averaged and complete topography cases are qualitatively similar, indicating that again the north-south slope is primarily causing the change in the Hadley cells. Dust has the effect of scattering light out of the solar beam; thus less solar f ux reaches the surface. The surface cools while the atmosphere heats, to the point of shutting off convection. This affect alone should reduce the effect of the north-south slope and produce more symmetric cells regardless of topography. However, Fig. 1 shows that for the zonally averaged and complete topographies the boundary has shifted far northward of the equator and that only the “southern” (i.e. counterclockwise) cell is present. Figure 2 shows the temperature for the same cases shown in Fig. 1. For the cases of nonzero topography and no dust, the temperature maximum is shifted (as compared to the case with no topography) from the subsolar point at the equator to the south due to greater convective heating over higher topography. For the case of nonzero topography and dust, the temperature maximum is shifted northward where the atmospheric column is deeper and there is more dust heating. This northward shift in the peak heating causes the boundary to also shift northward, and the counterclockwise cell to dominate.

For the case of nonzero dust, the temperature prof les develop an inversion at low and mid latitudes below ~7 km. The inversion is also present at the solstice seasons (not shown). Inversions are not typically seen in other models, except Basu et al. (2006) do show an inversion from L_s=285–315°. Wilson and Hamilton (1996) show in their MGCM at L_s=270° an increase in the vertical temperature gradient as dust loading is increased to a maximum solar optical depth at the surface of 1. The inversion in the Zalucha et al. (2010) MIT MGCM suggests that the effects of the dust heating are exaggerated here. Vertical mixing of heat is not included in the MGCM except for convective adjustment, which does not occur when large amounts of dust is present because the surface is cooler than the atmosphere in those cases. A simple gray IR scheme has been attempted to represent dust cooling, but success has not been achieved in moderating the inversion.

Conclusion

At equinox, increased dust loading causes the Hadley cell boundary to move northward, the southern cell to strengthen, and the northern cell to weaken as compared with the no dust case. As in the no dust case, the north-south slope is key in determining the characteristics of the Hadley cells, but in a different way that has two components. First, dust cools the surface, shutting off convection and decoupling the surface from the atmosphere. Second, the increased column depth over lower altitudes allows for more dust heating, shifting the peak dust heating northwards. This change in the meridional gradient in heating produces the observed changes in the model Hadley cells.

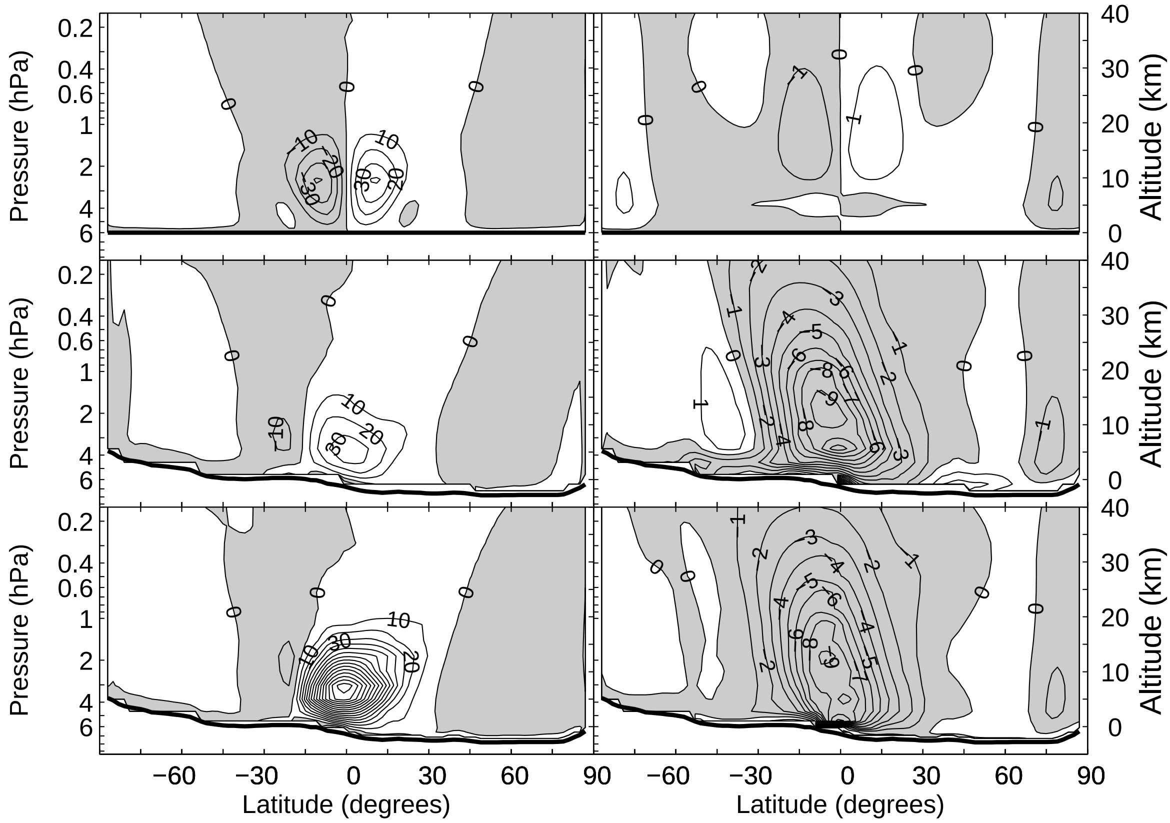

Figure 1: MGCM results for zonally and time averaged mass stream function. Units are 10^8 kg s^{-1}. Positive f ow is clockwise; negative contours are shaded. Only results below ∼0.2 hPa (40 km altitude) are shown. The left column is for no dust, and the right column is for a solar optical depth at the surface of 1. From top to bottom, the rows are f at, complete MOLA topography, and zonally averaged MOLA topography. Note the different contour intervals between the left and right columns.

Acknowledgments

I thank John Wilson for the dust scheme code and discussions regarding the effect of dust in the Martian atmosphere.

References

Adcroft, A. and J.-M. Campin, 2004: Rescaled height coordinates for accurate representation of free-surface f ows in ocean circulation models. *Ocean Modelling*, **7**, 269–284.

Adcroft, A., J.-M. Campin, C. Hill, and J. Marshall, 2004: Implementation of an atmosphere-ocean general circulation model on the expanded spherical cube. *Mon. Wea. Rev.*, **132**, 2845–2863.

Adcroft, A., C. Hill, and J. Marshall, 1997: Representation of topography by shaved cells in a height coordinate ocean model. *Mon. Wea. Rev.*, **125**, 2293.

Basu, S., J. Wilson, M. Richardson, and A. Ingersoll, 2006: Simulation of spontaneous and variable global dust storms with the GFDL Mars GCM. *J. Geophys. Res.*, **111**, E09 004, doi:10.1029/2005JE002660.

Briegleb, B. P., 1992: Delta-Eddington approximation for solar radiation in the NCAR community climate model. *J. Geophys. Res.*, **97**, 7603–7612.

Caballero, R., R. T. Pierrehumbert, and J. L. Mitchell, 2008: Axisymmetric, nearly inviscid circulations in non-condensing radiative-convective atmospheres. *Quart. J. Roy. Meteor. Soc.*, **134**, 1269–1285, doi: 10.1002/qj.271.

Conrath, B. J., 1975: Thermal structure of the Martian atmosphere during the dissipation of the dust storm of 1971. *Icarus*, **24**, 36–46, doi:10.1016/0019-1035(75)90156-6.

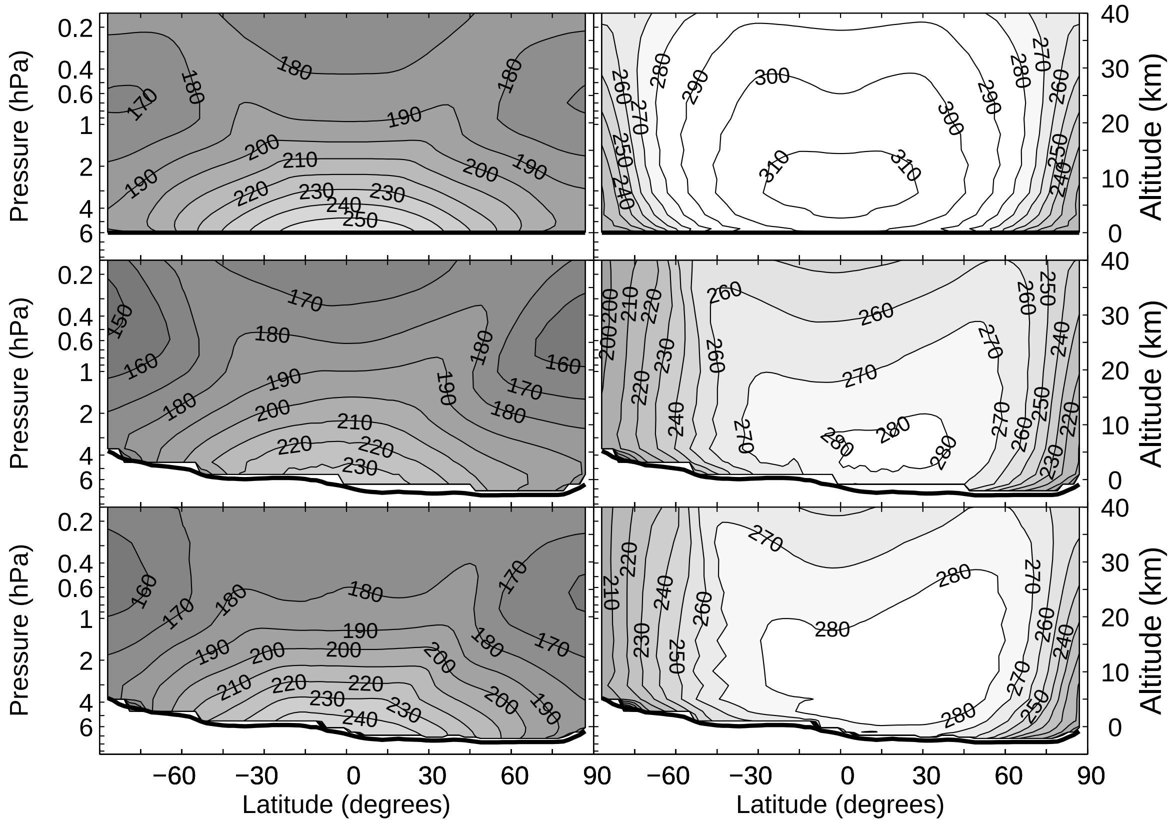

Figure 2: MGCM results for zonally and time averaged temperature. Units are K. Only results below ∼0.2 hPa (40 km altitude) are shown. The panels are ordered in the same way as Fig. 1.

Joshi, M. M., S. R. Lewis, P. L. Read, and D. C. Catling, 1995: Western boundary currents in the Martian atmosphere: Numerical simulations and observational evidence. *J. Geophys. Res.*, **100 (E3)**, 5485–5500.

Lindzen, R. S. and A. Y. Hou, 1988: Hadley circulations for zonally averaged heating centered off the equator. *J. Atmos. Sci.*, **45 (17)**, 2416–2427.

Marshall, J., A. Adcroft, C. Hill, L. Perelman, and C. Heisey, 1997: A f nite-volume, incompressible Navier Stokes model for studies of the ocean on parallel computers. *J. Geophys. Res.*, **102**, 5753–5766.

Pollack, J. B., D. S. Colburn, F. M. Flasar, R. Kahn, C. E. Carlston, and D. G. Pidek, 1979: Properties and effects of dust particles suspended in the Martian atmosphere. *J. Geophys. Res.*, **84**, 2929–2945, doi: 10.1029/JB084iB06p02929.

Richardson, M. I. and R. J. Wilson, 2002: A topographically forced asymmetry in the Martian circulation and climate. *Nature*, **416**, 298–301.

Smith, D. E., et al., 1999: The global topography of Mars and implications for surface evolution. *Science*, **284 (5419)**, 1495–1503.

Takahashi, Y. O., H. Fujiwara, H. Fukunishi, M. Odaka, Y.-Y. Hayashi, and S. Watanabe, 2003: Topographically induced north-south asymmetry of the meridional circulation in the Martian atmosphere. *J. Geophys. Res.*, **108 (E3)**, doi:10.1029/2001JE001638.

Wilson, R. J. and K. Hamilton, 1996: Comprehensive model simulations of thermal tides in the Martian atmosphere. *J. Atmos. Sci.*, **53 (9)**, 1290–1326.

Zalucha, A. M., R. A. Plumb, and R. J. Wilson, 2010: An analysis of the effect of topography on the Martian Hadley cells. *J. Atmos. Sci.*, **67**, 673–693, doi: 10.1175/2009JAS3130.1.